Pis'ma v ZhETF, vol. 92, iss. 7, pp. 507 – 512 © 2010 October 10

Shot noise measurements in a wide-channel transistor near pinch-off

V. S. Khrapai, D. V. Shovkun

Institute of Solid State Physics RAS, 142432 Chernogolovka, Russian Federation

Submitted 9 August 2010
Resubmitted 30 August 2010

We study a shot noise of a wide channel gated high-frequency transistor at temperature of 4.2 K near pinch-off. In this regime, a transition from the metallic to the insulating state is expected to occur, accompanied by the increase of the partition noise. The dependence of the noise spectral density on current is found to be slightly nonlinear. At low currents, the differential Fano factor is enhanced compared to the universal value 1/3 for metallic diffusive conductors. We explain this result by the effect of thermal fluctuations in a nonlinear regime near pinch-off, without calling for the enhanced partition noise.

A current I flowing in a two-terminal conductor placed in external electric circuit exhibits fluctuations around it's mean value $\overline{I}$. The second moment of the fluctuations is related to the noise spectral density $\overline{(I-\overline{I})^2}\Big|_{\Delta f} \equiv S_I\Delta f$, where Δf is a measurement bandwidth. In the absence of current ($\overline{I}=0$) the noise is related to thermal fluctuations of the occupation number of the electronic states, known as Johnson-Nyquist noise (JN-noise). In this case $S_I = 4k_BTR^{-1}$, where k_B, T and R are, respectively, the Boltzman constant, the temperature and the resistance of the conductor. Away from the equilibrium, when the voltage drop across the conductor is high enough $|eV| \gg k_BT$, and in the absence of dissipation inside the conductor and spurious noises, the current fluctuations are caused by the discreteness of the elementary charge e [1]. This noise is referred to as shot noise and for a voltage-biased conductor has a spectral density of $S_I = 2F|e\overline{I}|$, where F is called a Fano-factor.

In a non-interacting system in the linear transport regime, the shot noise is caused by a partition of incident carriers, which can be viewed as quantum effect [2]. In this case, the Fano-factor is determined by the distribution of the eigen-channel transparencies (T_n) of the conductor $F = \overline{T_n(1-T_n)}/\overline{T_n} \leq 1$ [2]. The noise is strongest ($F = 1$) in the Poissonian regime, which is obtained when all $T_n \ll 1$. In a quasi one dimensional metallic diffusive conductor the distribution of T_n is universal [3] and $F = 1/3$, which has been experimentally confirmed [4]. The universality of the value $F = 1/3$ in metallic conductors has been proven to be independent of geometry [5]. Near the transition from the metallic to the insulating state one expects an increase of the partition noise to the Poissonian value [2], although this regime haven't been studied experimentally.

We study the shot noise in a gated wide channel transistor near pinch-off, where the transition to the insulating state is expected to occur. The dependence of S_I on current is slightly non-linear in the shot noise regime. The differential Fano-factor $F_D = (2|e|)^{-1}|dS_I/dI|$ is enhanced above the universal metallic value $1/3 < F_D \leq 0.5$ for low $|I|$ and is close to this value $F_D \approx 1/3$ for higher $|I|$. We find that the enhancement of F_D is not necessarily related to the partition noise. In contrast, it can be explained by a classical effect of thermal fluctuations in a strongly nonlinear transport regime near pinch-off.

The sketch of the measurement is shown in Fig.1. The sample and the cryogenic amplifier (LTAmp) are

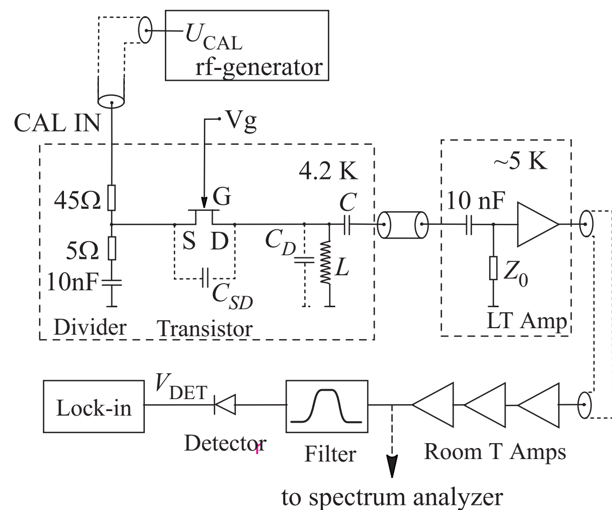

Fig.1. The sketch of the setup. The low temperature parts are shown by dashed boxes. The parameters of the resonant LC circuit and the undesired stray capacitances C_{SD} and C_D (shown by dashed lines inside the 4.2 K box) are given in the text. The signal from the room temperature amplifiers (Room T Amps) is either sent to the filter and detector for a Lock-in measurement or to the spectrum analyzer (dashed line with an arrow) for wide range spectra acquisition

placed in a ^{4}He gas chamber with the walls maintained at 4.2 K. The sample is below the LTAmp and is connected to it with a 20 cm long cable. A heat sink connects the LTAmp to a liquid ^{4}He bath. The actual temperature of the LTAmp (T_{LTA}) measured with a thermometer is about 5.3 K. The actual temperature of the sample is taken to be 4.2 K, consistent with the JN-noise measurement (see below). At the input of the setup (CAL IN) a 50 Ω cable is connected to the transistor source (S) via a divider. This input is used both for driving a current I and external rf calibration. A transistor drain (D) is followed by an $L-C$ resonator, which is connected to a cryogenic amplifier (LTAmp) (≈ 20dB gain). The resonator serves to match a high impedance of the sample and a low input impedance $Z_0 = 50\ \Omega$ of the LTAmp. The output of the LTAmp is connected via a second 50 Ω cable to the input stage of the room-temperature low-noise amplifiers (total gain of 3×20 dB). Finally, the amplified signal is filtered with a ~30 MHz bandpass filter at the resonance frequency $f_0 \approx 125$ MHz and rectified by a detector (8473C by Agilent Technologies). The ac modulation of the rectified signal thanks to a current modulation, gate voltage chopping or amplitude modulation of the external rf is measured with the lock-in. Alternatively, a spectrum analyzer can be used to analyze the frequency spectra at the output of the room-temperature amplifiers. We study shot noise of a commercial AlGaAs/InGaAs/GaAs pHEMT ATF-35143 by Agilent with a gate length (width) of 0.5 (400) μm. This transistor is known for low noise at room temperature and is used as an active element in cryogenic LTAmp's by us and other authors [6]. We preformed the resistance measurements in two such transistors (samples 1 and 2), and noise measurements and calibration only in sample 2.

Negative gate voltage $V_g < 0$ is used to deplete the channel which results in increase of the linear-response S-D resistance $R \equiv dV/dI|_{I\to 0}$. The huge aspect ratio of the gate electrode allows to work near the pinch-off with high channel resistivity in the range of MΩ/□ while keeping a reasonable R. The dependence $R(V_g)$ at 4.2 K is shown in the inset of fig.2 for sample 1 (solid line) and for several states of sample 2 (symbols). In all cases, the behavior $R(V_g)$ is roughly exponential and is reproducible up to insignificant random threshold voltage shifts (see caption). Hence, most likely, the current is homogeneously distributed across the transistor channel near pinch-off. Such a strong dependence $R(V_g)$ might indicate that we enter the insulating phase near the pinch-off [7]. The measured differential resistance $R_{\rm diff} \equiv dV/dI$ is shown as a function of current in fig.2a for three values of the gate voltage in sample 2. These data are taken simultaneously with the shot noise measurements presented below. $R_{\rm diff}$ is maximum in the linear response ($I = 0$) and falls down at finite current. The reduction of $R_{\rm diff}$ with current is most pronounced at low $|I|$ and for more depleted channel. $R_{\rm diff}$ is an asymmetric function of current, which is related to the capacitive population/depopulation of the channel at negative/positive bias. The nonlinear I-V curves numerically calculated from these data are plotted in fig.2b.

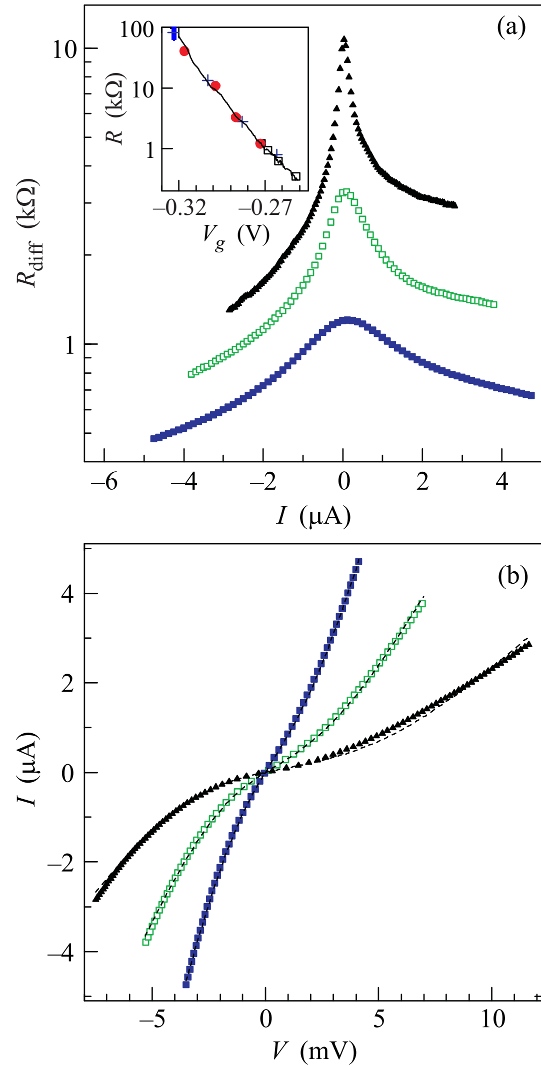

Fig.2. (a) Differential resistance $R_{\rm diff}$ as a function of current for three values of the gate voltage in sample 2. Inset – linear response S-D resistance as a function of gate voltage for sample 1 (solid line) and three different states of sample 2 (shown by different symbols). The V_g axis for different sample states was compensated for random shifts on the order of 50 mV. (b) Experimental I-V curves calculated from the data of (a) shown by the same symbols as the corresponding data for $R_{\rm diff}$ in (a). Model fits (see text) are shown by dashed lines

The nonlinearity is somewhat similar to the behavior of the I-V curves in the insulator breakdown regime [8], although much less pronounced, possibly because of the much higher temperature.

The main ingredient of the shot noise measurements is the calibration of the setup gain and bandwidth described below. A rectified voltage $V_{\rm DET}$ at the output of the detector is proportional to the power P incident on the detector. The power P is the sum of contributions P_T proportional to the transistor noise S_I^T, P_{Z_0} proportional to the input current noise of the LTAmp $S_I^{Z_0}$ and a constant contribution coming from the input voltage noise of the LTAmp and noises of all other amplifiers. The LTAmp's input current noise is dominated by the JN-noise of the input resistor $S_I^{Z_0} \approx 4k_BT_{LTA}/Z_0$. The actual noise temperature can be somewhat higher owing to extra current noise from the active parts of the LTAmp. Small noises from the two resistors at the input divider (fig.1) are neglected. Below we are interested only in a differential part of $V_{\rm DET}$ measured with a lock-in, which depends on the transistor S-D current I and/or its (linear or differential) S-D resistance. Hence, up to an unimportant constant one gets:

$$V_{DET}^{\rm noise} = D(P_T + P_{Z_0}) = S_I^T R^2 \cdot DG \int |k_T|^2 df + \\ + S_I^{Z_0} Z_0^2 \cdot DG \int |k_{Z_0}(f,R)|^2 df, \qquad (1)$$

where D is the detector power to voltage conversion coefficient, G – total power gain of the amplifiers divided by the input resistance Z_0. k_T and $k_{Z_0}(f,R)$ denote the voltage transfer functions of the corresponding noise sources to the input of the LTAmp, which both depend on f and R. The transfer functions are set by the parameters of the circuit in fig.1, which we determine via the following calibration procedure. We apply an rf signal of amplitude U_{CAL} at a frequency f to the input CAL IN (see fig.1) and measure the contribution V_{DET}^{CAL} to the output detector voltage. The detector signal is proportional to power P_{CAL} incident on the detector:

$$V_{DET}^{CAL} = DP_{CAL} = D|k_T'|^2 \cdot |k_{GEN}|^2 G \cdot U_{CAL}^2, \qquad (2)$$

where k_{GEN} is the voltage divider coefficient at the CAL IN input of the circuit (fig.1). k_T' is the rf-voltage transfer function, which is related to the noise transfer function k_T from eq. (1) as $|k_T'|^2 = \alpha |k_T|^2$. Factor $\alpha = 1 + 4\pi^2 f^2 R^2 C_{SD}^2$ accounts for the suppression of the transistor voltage noise caused by a stray S-D capacitance C_{SD}. The power P_{CAL} measured with a spectrum analyzer is shown in fig.3a as a function of f for a set of gate voltages (symbols). The quality factor of the LC-resonator in fig.1 increases with R, which results in narrower peak for more depleted channel in fig.3a. Solid lines represent the best fits to the data used to accurately determine the values of $L \approx 300$ nH, $C \approx 1.5$ pF, the drain-ground stray capacitance $C_D \approx 3.9$ pF and $C_{SD} \approx 0.2$ pF. We find that C_D is dominated by a stray capacitance of the hand-made inductor (L in fig.1) and the value of C_{SD} is close to an intrinsic parameter of the transistor. The quality of the fits is almost perfect, apart from small oscillations presumably caused by resonances in the rf-tract. These discrepancies are not important as they occur beyond the bandwidth used for noise measurements.

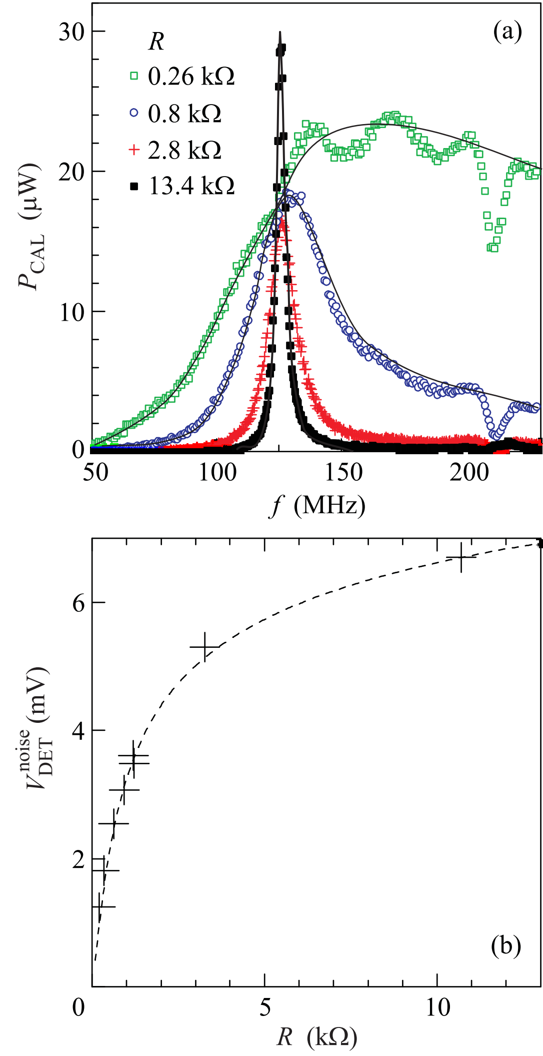

Fig.3. (a) Frequency response spectra of the setup at $I = 0$ acquired with a spectrum analyzer for a set of linear response resistances R indicated in the legend. Experimental data and fits are shown by symbols and lines, respectively. (b) Calibration of the setup via equilibrium noise measurement (see text). Symbols and line: measured chop amplitude of the detector voltage and fit, respectively

Fitting the data of fig.3a with eq. (2) returns the value of the product $|k_{GEN}|^2G$, whereas a separate knowledge of G is required for noise measurements. This is achieved via a measurement of the equilibrium noise of the setup, which depends on R (see eq. (1)). We chop the transistor gate voltage between the two values, corresponding to nearly zero ($\sim 10\Omega$) and finite R and measure the first harmonic ac component of the detector voltage $V_{DET}^{\rm noise}$ with a lock-in. The result is plotted in fig.3b as a function of R (symbols). The noise signal $V_{DET}^{\rm noise}$ increases as the transistor is depleting, which reflects the increase of the JN voltage noise of the transistor. The overall dependence is caused by the interplay of the R-dependent bandwidth of the resonant circuit and a (negative) contribution from the chopped LTAmp's input current noise. The experimental behavior is well captured by the dashed line fit in fig.3b. The fitting parameters include G, the LTAmp's input noise temperature of $T_{LTA} \approx 4.7\,$K and the sample temperature of $T = 4.2\,$K. Consistently, an independent thermometry returned the value of $\approx$5.3 K for the temperature of the resistor Z_0 (fig.1). Under assumption of $T_{LTA} = 5.3\,$K the best fit to the data of fig.3b would be obtained for a sample temperature of $\approx 4.8\,$K. This discrepancies represents a possible systematic error in our calibration and shot noise measurements, so that the Fano factor values given below may actually be within 10% higher.

As follows from fig.3, at $I = 0$ the rf-response of the transistor and its equilibrium noise are successfully described by a single stray capacitance parameter C_{SD}. We find that this is not the case under non-linear transport conditions. Presumably, the reason is the inhomogeneous electron density distribution below the gate at $I \neq 0$, which can change, e.g., distributed gate-drain and gate-source capacitances. Instead of introducing more fitting parameters at $I \neq 0$, we calibrate the noise transfer function k_T in-situ, with the help of the rf generator. According to eq. (2) integration of the frequency response of the setup to the external rf-signal gives:

$$DG \int |k_T|^2 df = (\alpha |k_{GEN}|^2 U_{CAL}^2)^{-1} \int V_{DET}^{CAL} df \quad (3)$$

The quantity $K_{CAL} \equiv DG \int |k_T|^2 df$ obtained in this way accounts for the I-dependent gain and bandwidth of the shot noise measurement in the nonlinear regime.

Using equations (1) and (3) the measurement of the shot noise spectral density S_I^T is straightforward. In the nonlinear regime the voltage noise of the transistor is determined by the differential resistance $R_{\rm diff}$ which substitutes R in eq. (1) and expression for factor α. The LTAmp's noise transfer function $k_{Z_0}(f, R)$ is evaluated with the known $I = 0$ circuit parameters and $R = R_{\rm diff}$. We measure the dc contribution to the detector voltage caused by finite S-D current $V_{DET}^{\rm noise}$. This is achieved via a lock-in measurement of the derivative dV_{DET}/dI and subsequent numeric integration. The integration constant is obtained via the equilibrium noise measurement (fig.3b). The (arbitrarily offset) result is shown in fig.4 for one value of V_g (see caption). Here, the dashed line

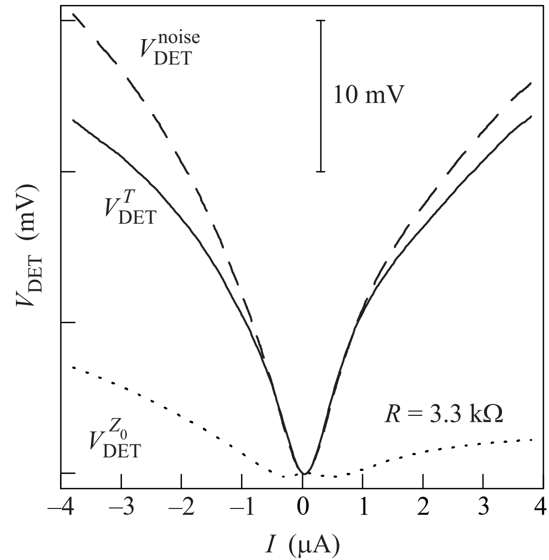

Fig.4. Integrated detector voltage $V_{DET}^{\rm noise} = V_{DET}^T + V_{DET}^{Z_0}$ as a function of S-D current (dashed line). Contributions from the transistor noise (V_{DET}^T) and input current noise of the LTAmp ($V_{DET}^{Z_0}$) are shown by solid and dotted lines, respectively. The data are taken for the same gate voltage as the traces shown by squares in fig.2 (linear-response resistance indicated in the figure)

is the experimental $V_{DET}^{\rm noise}$. The evaluated contribution of the LTAmp's input current noise $V_{DET}^{Z_0}$ is shown by dots. $V_{DET}^{Z_0}$ is not a constant, thanks to the $R_{\rm diff}$ dependence on I in the nonlinear regime, which slightly modifies the impedance connected to the input of the LTAmp. As seen from fig.2, $R_{\rm diff}$ changes stronger for $I < 0$, which results in a corresponding asymmetry of $V_{DET}^{Z_0}$ as a function of I in fig.4. The difference $V_{DET}^T = V_{DET}^{\rm noise} - V_{DET}^{Z_0}$ is the contribution thanks to transistor shot noise shown by solid line. The functional dependence of V_{DET}^T on I is related to that of the noise spectral density as $S_I^T = V_{DET}^T/(R_{\rm diff}^2 K_{CAL})$.

In figs.5a, b and 5c the noise spectral density S_I^T is plotted as a function of I for three values of the gate voltage (symbols). At $I = 0$ the noise spectral density is minimum and equals the JN value. At $I \neq 0$, S_I^T increases as a function of $|I|$ and demonstrates a nearly linear behavior at high enough currents. We find that for all experimental traces, in the

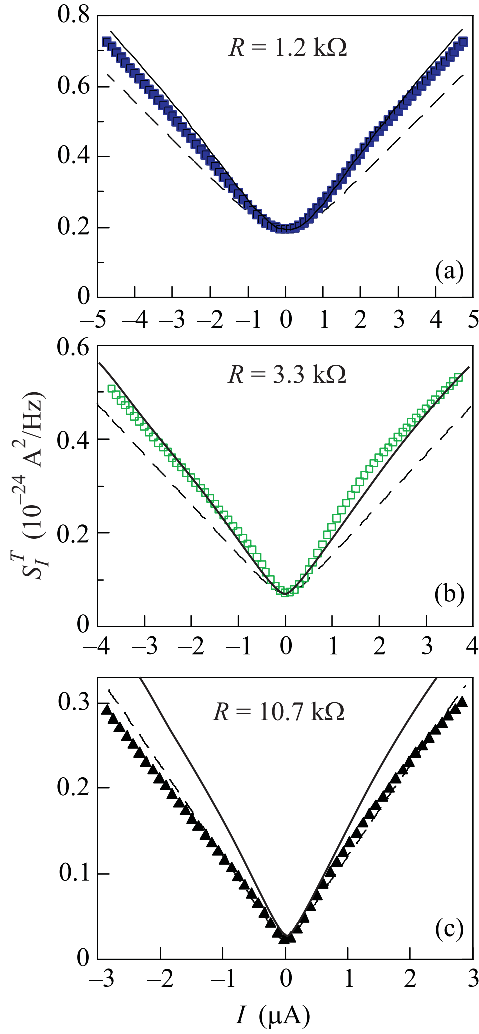

Fig.5. Shot noise spectral density S_I^T as a function of S-D current for three values of the gate voltage (linear-response resistance R shown in the figures). Experimental data in (a),(b),(c) are measured simultaneously with the data of fig.2 and are shown by the respective symbols. Dashed lines are fits to the standard linear response shot noise formula [4]. Solid line are fits according to eq. (4) and a model of nonlinear transport described in the text

limit of high currents, the differential Fano-factor is close to the universal value $F_D \approx 1/3$. For comparison, we plot S_I expected for a metallic diffusive conductor in the linear regime by dashed lines in fig.5. These lines are drawn according to the standard formula $S_I = \frac{2}{3}R^{-1}\left[4k_BT + |eV|\coth(|eV|/2k_BT)\right]$, where R is the experimental linear response resistance and V is the associated voltage drop $V = IR$ [4]. The symbols in figs.5a and 5b (obtained for a less depleted transistor) are systematically above the dashed lines, i.e. for the same I the noise spectral density exceeds the one obtained with the above formula. Hence, at low currents the differential Fano-factor is enhanced compared to 1/3, which is most pronounced for the data in fig.5b with $F_D \approx 0.5$ for $|I| \sim 1\mu$A. This discrepancy is beyond the experimental uncertainty and can be explained by the effect of thermal fluctuations in the nonlinear transport regime, as we propose below.

The general result for shot noise spectral density of a two-terminal conductor is usually express in terms of the energy-dependent 1D eigen-channel transparencies $T_n(E)$ [2]. For the case of wide channel transistor, it is convenient to express the same result in terms of the energy-dependent conductance $\sigma(E) = e^2/h\sum T_n(E)$, where h is the Planck's constant, and the Fano-factor of the partition noise $F = \overline{T_n(1-T_n)}/\overline{T_n}$:

$$S_I = 2\int \sigma(E)dE\{f_L(1-f_L) + \\ +f_R(1-f_R) + F(f_L - f_R)^2\} \quad (4)$$

Here, $f_i = (1+\exp[(E-\mu_i)/k_BT])^{-1}$ are the Fermi distributions of the left ($i = L$) and right ($i = R$) reservoirs, with respective electrochemical potentials of $\mu_i = \pm|e|V/2$. The first two terms in the integrand of eq. (4) represent the thermal noise of the reservoirs, while the last term stands for the shot noise. Eq. (4) provides a phenomenological description of the shot noise behavior in the nonlinear regime. We find that the experimental enhancement of the differential Fano-factor $F_D > 1/3$ (fig.5a and 5b) is not necessarily related to energy dependence of F. Below we assume that the partition noise Fano-factor in the last term of eq. (4) has a universal value $F = 1/3$ for metallic diffusive conductors independent of energy.

The energy dependent conductance $\sigma(E)$ is directly related to the transport current as $I = |e|^{-1}\int\sigma(E)(f_L - f_R)dE$ and can be obtained by fitting the experimental I-V curves (fig.2b). We model $\sigma(E)$ by a step-like functional dependence on energy $\sigma(E) = \sigma_0(1+\tanh[(E - E_0 - \lambda|e|V)/\Delta])$. Parameters $\sigma_0 \sim 10^{-2}\Omega^{-1}$ and $E_0, \Delta \sim 1$ meV define the shape of the conductance step, whereas the parameter $\lambda \sim 0.1$ accounts for the asymmetry of the I-V curves (fig.2b) thanks to capacitive effects of finite bias. This conductance model was chosen for its analogy to the step-like behavior of the density of states near the metal-insulator transition in two dimensions [7]. Fig.2b demonstrates that the model provides good fits (dashed lines) to the experimental nonlinear I-V curves (symbols). The so-obtained $\sigma(E)$ and eq. (4) predict the behavior of the noise spectral density, which is shown by solid lines in fig.5.

The enhancement of the differential Fano-factor in a less depleted channel at small I (symbols in figs.5a

and 5b) is qualitatively captured by the fits according to eq. (4) (solid lines). Note, that thanks to assumption of $F = 1/3$ the eq. (4) reduces to $S_I = 2/3|eI|$ at $T = 0$. In other words, within our model the enhancement of $F_D > F = 1/3$ is a finite temperature effect. The finite temperature determines the thermal fluctuations in the electron flow incident on the conductor. In the nonlinear regime, the contribution of thermal fluctuations to the current noise increases as a function of I, thanks to the energy dependence of the conductance $\sigma(E)$. This results in enhanced differential Fano-factor $F_D > F = 1/3$. Note, that this nonlinear effect is not related to a thermalization of the non-equilibrium carriers inside the conductor [9] or in the reservoirs [4].

The importance of the thermal fluctuations is best illustrated in the ultimate case of thermally activated conductance in the insulating phase, which in our model is achieved for $E_0, \Delta \gg T$. This is expected to occur in a strongly depleted transistor. Here, the eq. (4) predicts $F_D = 1$ at low $|I|$. In this case, the Poissonian value of the Fano-factor is caused by a classical reason that the occupation number of the current carrying states is small $f_i(E \sim E_0) \ll 1$ $(i = L, R)$. This is fully analogous to the case of the shot noise for thermionic emission in a vacuum tube considered by Schottky [1], and is not related to particular properties of the model we used for $\sigma(E)$. In the limit of high currents, the eq. (4) predicts a crossover to the partition noise in the insulator breakdown regime with $F_D \to F$. Unfortunately, we could not observe such a behavior experimentally. Fig.5c shows the noise spectral density for the lowest gate voltage (symbols), where the non-linearities are most pronounced (same symbols in fig.2). Unlike the prediction of eq. (4) (solid line), $F_D \approx 1/3$ and the data falls close to the standard metallic linear-response result (dashed line). Note, however, that at low $|I|$ this behavior might be an artefact caused by the uncertainty in the voltage noise suppression factor α, which is most crucial for measurements at high $R_{\text{diff}} \gtrsim 3k\Omega$.

In summary, we performed the shot noise measurements in a commercial high-frequency transistor near pinch-off. The dependence of the shot noise on current is slightly nonlinear. The differential Fano-factor is about $F_D \approx 1/3$ in the limit of high currents, and somewhat enhanced above the universal metallic value at lower currents $1/3 < F_D < 0.5$. The model of nonlinear transport near the pinch-off is suggested, which allows to explain the results in terms of classical effect of thermal fluctuation, without assuming the enhancement of the partition noise.

We acknowledge the discussions with A.A. Shashkin, V.T. Dolgopolov and V.F. Gantmakher. Financial support by RFBR, RAS, Ministry of Science and the grant # MK-3470.2009.2 is gratefully acknowledged. VSK acknowledges support from the Russian Science Support Foundation.

1. W. Schottky, Ann. Phys. (Leipzig) **57**, 541 (1918).
2. Ya .M. Blanter, M. Büttiker, Phys. Rep. **336**, 1 (2000).
3. C. W. J. Beenakker, Rev. Mod. Phys. **69**, 731 (1997).
4. M. Henny, S. Oberholzer, C. Strunk, and C. Schönenberger, Phys. Rev. B **59**, 2871 (1999).
5. Yu. V. Nazarov, Phys. Rev. Lett. **73**, 134 (1994).
6. L. Roschier and P. Hakonen, Cryogenics **44**, 783 (2004).
7. T. Ando, A.B. Fowler, and F. Stern, Rev. Mod. Phys. **54**, 437 (1982).
8. A. A. Shashkin, V. T. Dolgopolov, G. V. Kravchenko et al., Phys. Rev. Lett. **73**, 3141 (1994).
9. K. E. Nagaev, Phys. Rev. B **52**, 4740 (1995).